Rise in defibrillation threshold after postoperative cardiac remodeling in a patient with severe Ebstein's anomaly

Reina Bianca Tan, MD,* Charles Love, MD, FHRS,† Dan Halpern, MD,† Frank Cecchin, MD*

*From the *Division of Pediatric Cardiology, New York University Langone Medical Center, New York, New York, and †Division of Cardiology, New York University Langone Medical Center, New York, New York.*

Introduction

Implantable cardioverter-defibrillators (ICDs) are considered standard of care for patients with life-threatening cardiac arrhythmias. In small children and patients with venous anatomy that prohibits placement of traditional transvenous leads, nontransvenous coil positions have been used and can be characterized as epicardial, pleural, subcutaneous, or a hybrid of any of the 3 positions.[1–3] Based on the critical mass hypothesis, the defibrillation threshold is attained when a sufficient mass of excitable cells are simultaneously depolarized, which interrupts activation wavefronts.[4] Defibrillation is thus dependent on reaching a threshold current density in the myocardium. In transthoracic defibrillation, the magnitude of myocardial current density is dependent on the transcardiac current fraction (Fc), which is the ratio of the transcardiac threshold current (I_C) to the transthoracic threshold current (I_T). Over 95% of the transthoracic current is shunted by the thoracic cage and the lungs, with approximately 4% of the current traversing the heart.[5] Rise in defibrillation threshold may be due to use of certain medications, electrolyte abnormalities, underlying cardiac disease, ischemia, or increase in tranthoracic threshold current. We report a case of rise in defibrillation threshold associated with cardiac remodeling after surgical repair in a patient with Ebstein's anomaly.

Case report

A 22-year-old man with Ebstein's anomaly presented with cardiac arrest due to ventricular fibrillation. After successful resuscitation, cardiac magnetic resonance imaging (MRI) revealed Ebstein's anomaly with severe tricuspid valve regurgitation, massively dilated functional right ventricle (right ventricular end-diastolic volume [RVEDV] 855 mL, RV end-diastolic volume index [RVEDVI] 472 mL/m^2) and right atrium with atrialized right ventricle (right atrial volume [RAV] 693 mL, right atrial volume index [RAVI] 383 mL/m^2), and reduced biventricular systolic function (Figure 1A). An electrophysiology study was done and he had easily inducible monomorphic ventricular tachycardia with a cycle length of 300 msec, which was terminated with antitachycardia pacing. He underwent bidirectional Glenn, plication of atrialized right ventricle, right atrial reduction, placement of a 29-mm Mosaic valve, and ICD placement. Bidirectional Glenn precluded the use of the upper-extremity venous system, so we opted for an epicardial ICD system. A 25-cm coil was placed at the posterior aspect of the left ventricle (epicardial left ventricular lead [eLV]) and a 5-cm coil lateral to the right superior vena cava (epicardial superior vena cava lead [eSVC]). The generator was placed in a pocket posterior to the rectus sheath slightly leftward from midline. Defibrillation threshold (DFT) testing was performed 5 days after cardiopulmonary bypass. On testing, there was failure to convert with maximal output of 41 J. The system was then revised by adding a 25-cm coil from the left fifth mid-axillary line and tunneled subcutaneously toward the spine (Figure 2A). The eLV was connected to the subcutaneous (SC) coil using a Y adapter. DFT was performed with eLV/SC-eSVC coil configuration. Three inductions were done with this configuration, with failure at 31 J and success × 2 at 36 J, with a shock impedance of 36 Ω. During follow-up 2 months later, a significant reduction in cardiac size was noted on chest radiograph (Figure 1B). Since we had a 5 J safety margin for the DFT at implant, we proceeded to repeat DFT testing, which showed an increase in DFT to greater than 41 J and a decrease in shock impedance to 27 Ω. Cardiac computerized tomography (CT) scan was obtained, which showed a significant reduction in heart size (RV plus RA total volume decreased by 51%), resulting in an increase in the amount of lung between the SC coil and myocardial mass

KEYWORDS Arrhythmia; Ventricular fibrillation; Implantable cardioverter-defibrillator; Computerized tomography (CT); Magnetic resonance imaging (MRI) (Heart Rhythm Case Reports 2017;3:302–305)

Address reprint requests and correspondence: Dr Reina Bianca Tan, Division of Pediatric Cardiology, New York University Langone Medical Center, 403 East 34th Street, 4th Floor, New York, NY 10016. E-mail address: reinabianca@gmail.com; reina.tan@nyumc.org.

http://dx.doi.org/10.1016/j.hrcr.2017.03.007

KEY TEACHING POINTS

- Defibrillation threshold in nontransvenous implantable cardioverter-defibrillator (ICD) coil systems is determined by the ratio of transcardiac and tranthoracic current distribution.
- Cardiac remodeling can alter the transthoracic current distribution and raise the defibrillation threshold.
- Hybrid ICD coil placement is an alternative for pediatric patients and those with congenital heart disease.

(RVEDV 600 mL, RVEDVi 333 mL/m^2, RAV 160 mL, RAVI 89 mL/m^2) (Figure 2B). SC coil position was revised by moving the distal half of the coil from the posterior position to a more anterior and lateral location (Figure 2C). The device pocket was not opened. The lowest effective defibrillation threshold was 31 J, with a shock impedance of 46 Ω.

Discussion

In our patient, extensive remodeling of the right ventricle after surgical repair resulted in a decrease in cardiac volume with concomitant re-expansion of the left lung. This likely led to shunting of the current across the lung, leading to a drop in the impedance and increased DFT. Prior experiments have shown that 14% of the transthoracic current is shunted by the lung during transthoracic defibrillation.[6] Newman and colleagues[7] assessed the time-dependent effects with a transvenous defibrillation system and found that the impedance rises during follow-up. At our 2-month follow-up, we noted a 25% decrease in impedance rather than a rise as was expected. On repositioning of the subcutaneous coil, the impedance rose by 70%.

Jolley and colleagues[8] used a finite element model to demonstrate that defibrillation threshold testing variability is accounted for by electrode location and length of electrode coils. Using a transverse cut of a chest MRI and CT with the largest proportion of myocardium visible, the center of a circle around the myocardium was chosen as the center of the myocardial mass (Figure 1). Efficacy is improved by aligning the inter-electrode shock vector as closely as possible to the center of the mass of the ventricular myocardium, and by use of longer electrode coil lengths.[8] In our patient, the initial 2-epicardial-coil configuration did not cover the myocardial mass on the left chest and failed to depolarize a sufficient amount of fibrillating myocardium to terminate fibrillation. Implantation of an additional subcutaneous coil posterolaterally shifted the shock vector leftward and decreased the DFT.

Cardiac remodeling resulted in a reduction in posterior myocardial mass and redistribution of the intrathoracic current, as evidenced by the impedance drop. The CT demonstrated that the center of the myocardial mass moved anteriorly. Moving the coil anteriorly brought the coil closer to the center of the myocardial mass and reduced the amount of lung between the coil and myocardial mass. This resulted in a better electrode-to-generator shock vector, rise in impedance, and lowering of the DFT.

In patients with congenital heart disease and severe cardiomegaly, aligning the shock vector to the center of the mass is critical to achieving an acceptable defibrillation threshold. Remodeling of the heart post repair must be kept in mind, as this can change the DFT significantly in patients with nontransvenous ICD leads.

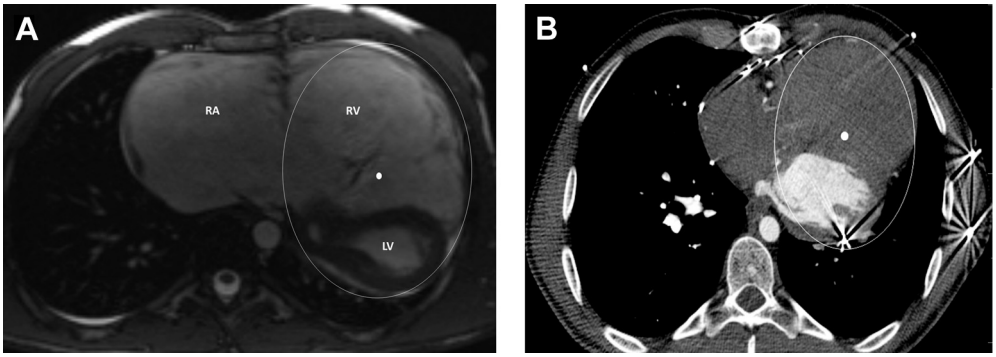

Figure 1 **A:** Preoperative cardiac magnetic resonance image of the heart. Center of myocardial mass is depicted as the center of an oblong around the myocardium and located at the midpoint of the left hemithorax. Severely dilated right atrium (RA) and right ventricle (RV) with posterior displacement of left ventricle (LV). **B:** Computerized tomography image of the heart 2 months post repair. Decreased RV size with re-expansion of left lung. The center of myocardial mass is shifted anteromedially compared to preoperative scan. eLV = epicardial left ventricular lead; SC = subcutaneous coil.

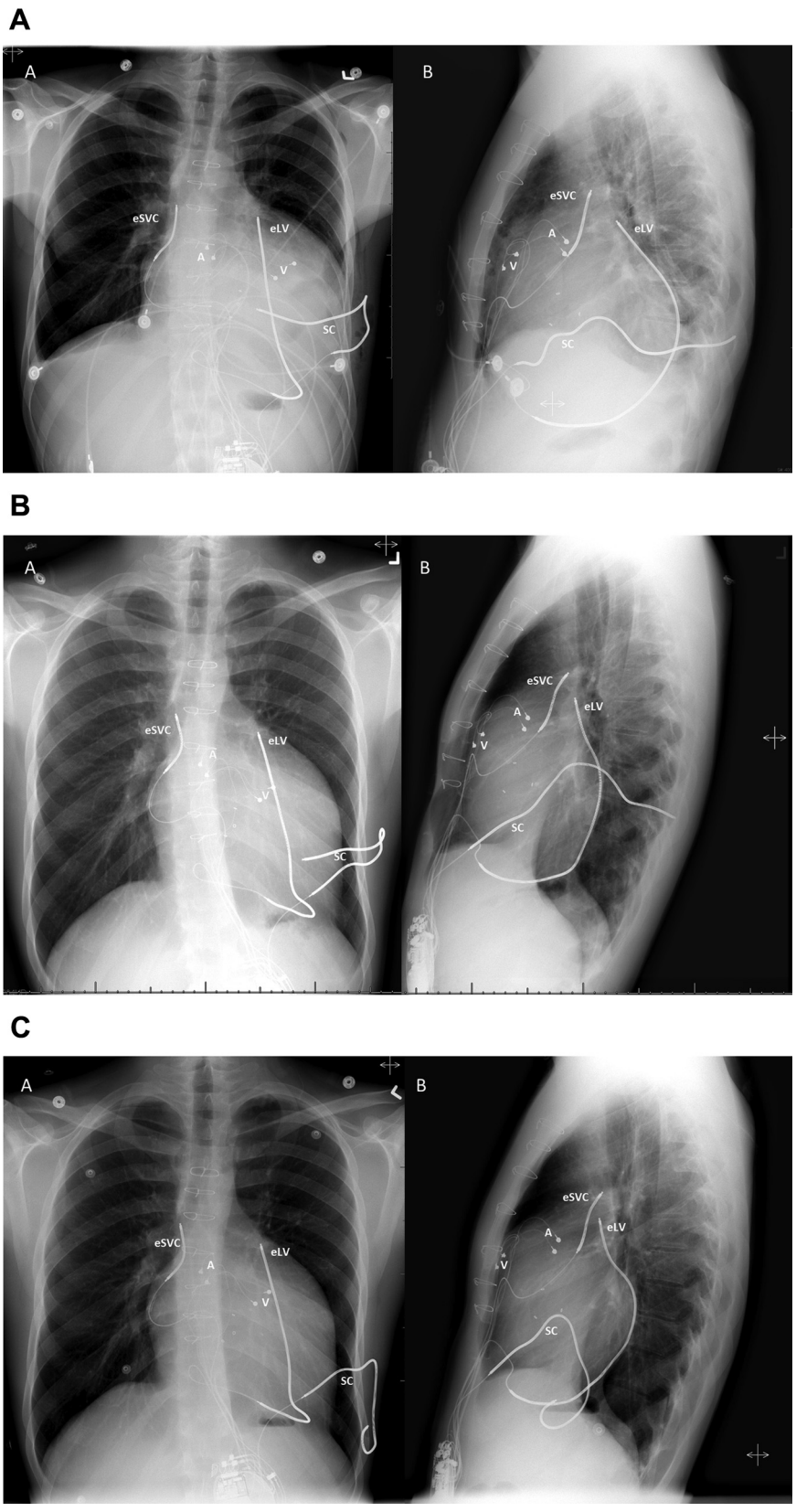

Figure 2 **A:** Early postoperative chest radiograph with an epicardial superior vena cava lead (eSVC), posterior epicardial left ventricular lead (eLV), subcutaneous array around the left hemithorax, and an abdominal generator. **B:** Chest radiograph 2 months post repair with decrease in heart size and re-expansion of left lower lung with relative shift of subcutaneous coil in relation to the heart. **C:** Chest radiograph post revision with stable epicardial SVC lead and posterior eLV lead and subcutaneous array around the anterior and left hemithorax. A = atrial lead; SC = subcutaneous coil; V = ventricular lead.

References

1. Stephenson EA, Batra AS, Knilans TK, et al. A multicenter experience with novel implantable cardioverter defibrillator configurations in the pediatric and congenital heart disease population. J Cardiovasc Electrophysiol 2006;17:41–46.
2. Berul CI, Triedman JK, Forbess J, Bevilacqua LM, Alexander ME, Dahlby D, Gilkerson JO, Walsh EP. Minimally invasive cardioverter defibrillator implantation for children: an animal model and pediatric case report. Pacing Clin Electrophysiol 2001;24:1789–1794.
3. Bardy GH, Smith WM, Hood MA, et al. An entirely subcutaneous implantable cardioverter-defibrillator. N Engl J Med 2010;363:36–44.
4. Zipes DP, Fischer J, King RM, Nicoll A deB, Jolly WW. Termination of ventricular fibrillation in dogs by depolarizing a critical amount of myocardium. Am J Cardiol 1975;36:37–44.
5. Lerman BB, Deale OC. Relation between transcardiac and transthoracic current during defibrillation in humans. Circ Res 1990;67:1420–1426.
6. Deale OC, Lerman BB. Intrathoracic current flow during transthoracic defibrillation in dogs. Transcardiac current fraction. Circ Res 1990; 67:1405–1419.
7. Newman D, Barr A, Greene M, Martin D, Ham M, Thorne S, Dorian P. A population-based method for the estimation of defibrillation energy requirements in humans : assessment of time-dependent effects with a transvenous defibrillation system. Circulation 1997;96:267–273.
8. Jolley M, Stinstra J, Tate J, Pieper S, Macleod R, Chu L, Wang P, Triedman JK. Finite element modeling of subcutaneous implantable defibrillator electrodes in an adult torso. Heart Rhythm 2010;7: 692–698.